

5'-CTAGGCCTGGAGGCCAGGTT-3' and R:
 5'-ACCCTGGAGTATGCGGGTTT-3' for ATF6; F:
 5'-ATCGAGTTCACCGAGCAGAC-3' and R:
 5'-TCACAGCTTTCTGGTCATCG-3' for PDI; F:
 5'-GGTCTGGTTCCTTGGTTTCA-3' and R:
 5'-TTCGCTGGCTGTGTAAGTTG-3' for PERK; F:
 5'-ACATCAAATGGGGTGATGCT-3' and R:
 5'-AGGAGACAACCTGGTCCTCA-3' for peptidylprolyl
 isomerase A (PPIA); and F:
 5'-AAACAGAGTAGCAGCTCAGACTGC-3' and R:
 5'-TCCTTCTGGGTAGACCTCTGGGAG-3' for the X-box
 binding protein 1 (XBP1). The intensities of RT-PCR bands
 were quantified using the ImageJ program.

Western blot analysis

PCCL3 cells were lysed using RIPA buffer (25 mM Tris-HCl pH 7.6, 150 mM NaCl, 1% NP-40, 1% sodium deoxycholate, 0.1% SDS, 1 mM PMSF). To measure total protein concentration, the Pierce® BCA Protein Assay Kit (Thermo Scientific, Catalog no. 23225) was used. Proteins were separated by SDS-polyacrylamide gel electrophoresis and transferred to a nitrocellulose membrane. The resulting membrane was incubated with primary antibodies overnight at 4°C and then with the secondary antibody. Blots were developed using an enhanced chemiluminescence Western blotting detection system Kit (Amersham, Sweden). All antibodies were obtained from Santa Cruz Biotechnology (Santa Cruz, CA, USA).

XBP-1 splicing experiment

Total RNA was reverse transcribed, and double-strand cDNA was synthesized by PCR using sense and anti-sense primers specific from the XBP1 gene (F: 5'-AAACAGAGTAGCAGCGCAGACTGC-3', R: 5'-TCCTTCTGGGTAGACCTCTGGGAG-3'). The amplified cDNA was treated with *Pst*I, and the resulting products were analyzed by electrophoresis on a 2% agarose gel.

Enzyme-linked immunoassay (ELISA)

Amounts of T4 released into PCCL3 culture medium were determined using the rat T4 ELISA Kit-LS-F28089 (LSBio Co., WA, USA) following the manufacturer's instructions. Absorbance was measured at 405 nm using an EL-311 ELISA microplate reader.

Hoechst 33342 staining

Following treatment with Tpen, PCCL3 cells were incubated for 30 min with Hoechst 33342 loading dye (Molecular Probes; Thermo Fisher Scientific, Inc.) and washed three times in ice-cold 1 × PBS. Following staining for 10 min, the stained cells were monitored using a fluorescence microscope (Axio Scope A1; Zeiss GmbH, Jena, Germany) at 340 nm.

Statistical analysis

Statistical significance among multiple groups was assessed using one-way analysis of variance) test. All statistical analyses were performed using the GraphPad Prism 6 software (GraphPad Software Inc.). The data were presented as mean ± standard error of the mean. Each group contained six samples (n = 6). Differences were considered statistically significant for p < 0.05.

III. RESULTS AND DISCUSSION

Zinc is a bivalent ion essential for life [1]. Although it is, after iron, the second most needed metal in the human body, its mechanisms of action to promote survival are poorly known [2-4]. Recently, zinc deficiency has been reported in the elderly as the main cause of palate disorders, immune and metabolic dysfunctions, and pressure ulcers, leading to poor quality of life [38]. Thus, adequate serum levels of zinc need to be maintained for a healthy life [39]. Here, we investigated whether zinc deficiency induced ER stress signals and its effects on the secretion of Tg, a precursor of thyroid hormones, in PCCL3 cells.

Morphological differences in PCCL3 cells, including many cells floating in the medium, were observed after treatment with 10 μM Tpen (data not shown). Tpen toxicity for PCCL3 cells was tested by MTT assay after 4, 8, and 16 h of treatment with 1, 2.5, 5, 8, and 10 μM Tpen (Fig. 1A). The viability was slightly increased in the 4 h treatment group compared with that of untreated controls regardless of Tpen concentration, whereas it was slightly decreased for cells treated with 8 and 10 μM Tpen for 8 h. Additionally, the viability of PCCL3 cells treated 10 h with 5, 8, or 10 μM Tpen was lower and reached 70% of the control cell viability for Tpen concentrations of 8 and 10 μM. This finding indicated that Tpen high concentrations (greater than 8 μM) and long treatment time (longer than 8 h) led to cell death. These data were taken into consideration when selecting Tpen concentration and treatment time in the following experiments.

Next, we tested the effect of zinc depletion induced by Tpen on the gene expression of ER chaperones (PDI and BiP) and three ER transmembrane signaling proteins (PERK, IRE1, and ATF6) (Fig. 1B). Zinc depletion had no significant effect on BiP and PDI gene expression. In contrast, treatment with 8 μM Tpen for 4 h induced an increase of IRE1 expression by approximately 2.5 times, of PERK by approximately 1.75 times, and of ATF6 expression by approximately 1.25 times. Overall, the results of Fig. 1B indicated that the gene expression of the ER chaperones were not affected by zinc depletion induced

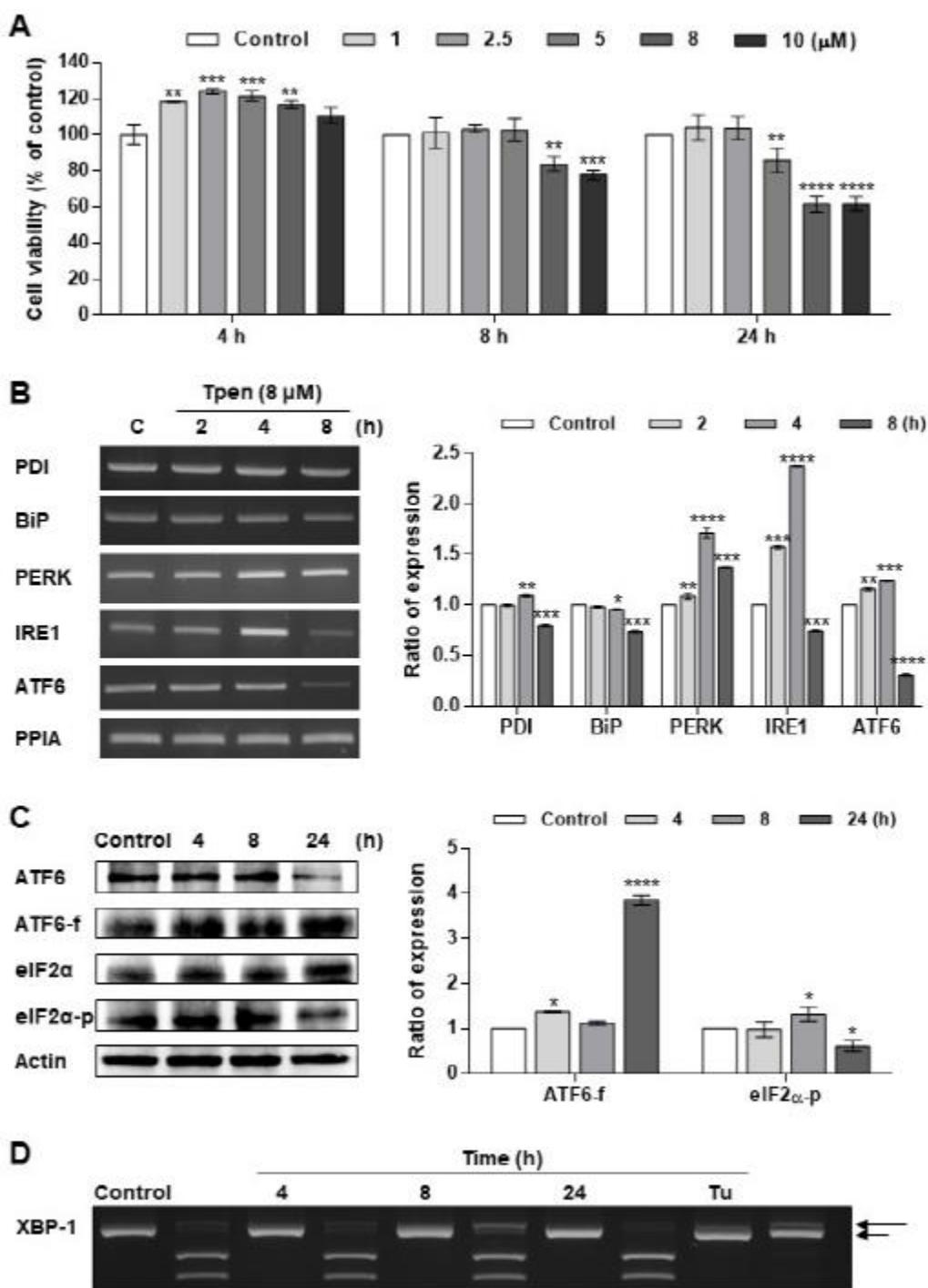


Figure 1. Cell viability and ER stress response after Tpen treatment. (A) PCCL3 cell viability was measured using MTT assays after treatment with different Tpen concentrations (1, 2.5, 5, 8, and 10 μ M) and for different durations (4, 8, and 24 h). (B) Induction of ER chaperones (PDI and BiP) and three ER transmembrane signaling proteins (PERK, IRE1, and ATF6) measured by RT-PCR. PPIA was used as the loading control. (C) Detection of ATF6 fragmentation (ATF6-f) and eIF2- α phosphorylation (eIF2 α -p) by western blot. (D) Detection of XBP1 mRNA splicing (the spliced XBP1 mRNA is indicated by an arrowhead), respectively. Data represent mean \pm standard error of the mean, $n = 6$, * $p < 0.05$, ** $p < 0.005$, *** $p < 0.001$, **** $p < 0.0001$ compared with controls.

Tpen in the thyroid cell line, whereas that of the ER transmembrane signaling proteins was regulated. These three ER transmembrane signaling proteins are involved in the UPR induced by the accumulation of unfolded or misfolded proteins in the ER lumen [21]. PERK is a type I transmembrane protein

kinase inhibiting total protein translation by phosphorylating eIF2 upon ER stress. Phosphorylated eIF2 structurally interferes with the formation of complexes required for protein translation [40]. ATF6 is an ER membrane-type II protein cleaved by site-1 and site-2 proteases (S1P and S2P) at its

cytoplasmic N-terminus to free its cytosolic domain, ATF6c, upon ER stress. ATF6c acts as a transcription factor to stimulate the gene expression of ER chaperones and ER-associated protein degradation (ERAD)-related genes [41]. IRE1 is autophosphorylated upon ER stress to induce XBP mRNA splicing, by cleaving XBP mRNA, generating an activated form of XBP1 mRNA that can be translated into XBP1 protein. XBP1 is a transcription factor upregulating the expression of UPR target genes associated with protein folding,

ER quality control, and ERAD [42]. Therefore, we investigated UPR signaling upon zinc depletion. ATF6c fragmentation was increased by approximately four times after 24 h of Tpen treatment, and eIF2- α phosphorylation was increased by approximately 1.5 times after 8 h of treatment (Fig. 1C). Additionally, alternative XBP cleavage was detected after 8 h treatment (Fig. 1D, arrowhead). Overall, these data suggested that although zinc depletion did not induce ER chaperone gene expression, zinc depletion activated factors downstream ER transmembrane signaling proteins.

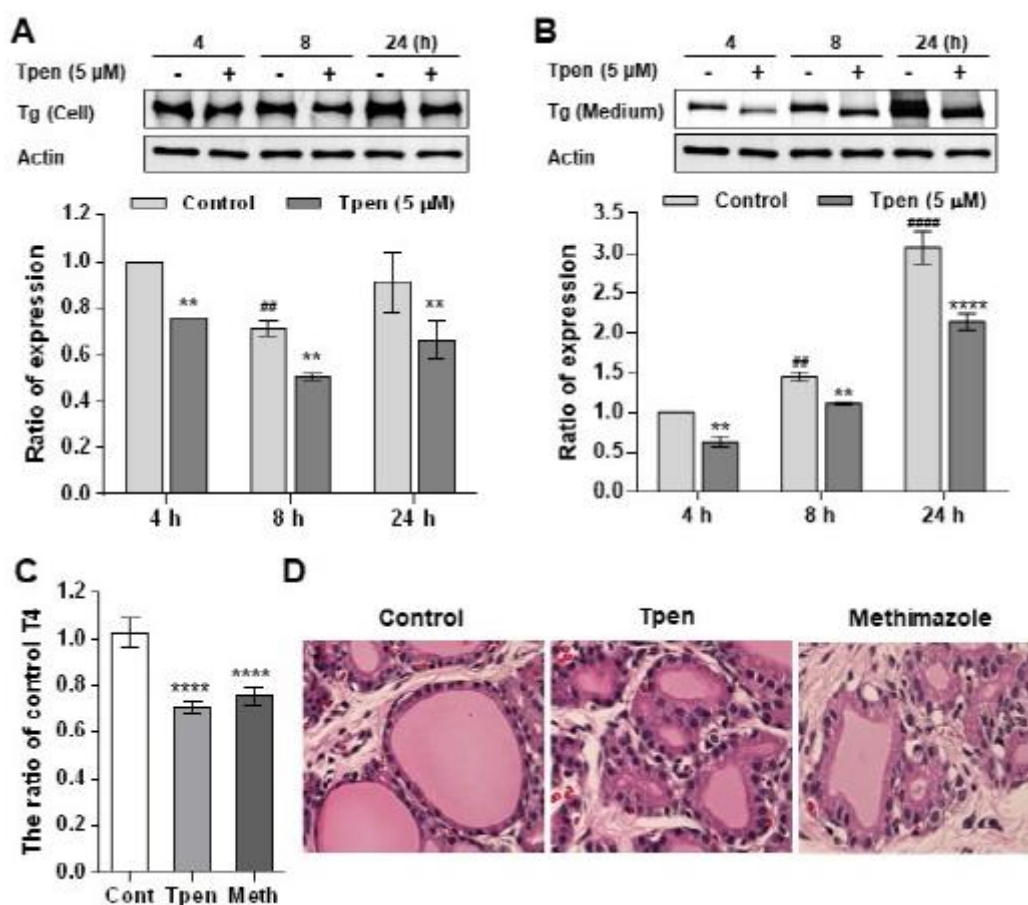


Figure 2. Tg biosynthesis and secretion upon Tpen treatment. (A) Intracellular Tg levels. PCCL3 cells were lysed after Tpen treatment for various durations (4, 8, and 24 h), and western blot using an anti-Tg antibody was performed. Band intensities were quantified and expressed as the ratio of the intensity in the control (not treated for 4 h). (B) Tg levels secreted in the culture medium. Here, the supernatant was subjected to western blot analysis as described above. (C) After 24 h of Tpen treatment, T4 levels secreted by PCCL3 were assessed by ELISA. (D) Thyroid tissue stained with hematoxylin-eosin under the same conditions as C ($\times 150$). Data represent mean \pm standard error of the mean, $n = 6$, * $p < 0.05$, ** $p < 0.005$, *** $p < 0.001$, **** $p < 0.0001$ compared with controls (not treated of each time point), ## $p < 0.005$, #### $p < 0.0001$ compared with the control of the 4-h time point. Met: methimazole.

Because zinc depletion affected UPR signaling protein expression, we assessed whether the intracellular biosynthesis and extracellular secretion of Tg were regulated by zinc depletion in PCCL3 thyrocytes. PCCL3 cells were treated with a nontoxic concentration of Tpen (5 μ M) for 4, 8, and 24 h, and the amounts of intracellular and secreted Tg were measured by western blot using an anti-Tg antibody. As shown in Fig. 2A, intracellular levels of Tg were approximately 80% lower after 8

and 24 h of Tpen treatment than those in controls and cells treated for 4 h. The levels of Tg secreted from the cells were decreased after Tpen treatment to 60%, 70%, and 65% of the control levels after 4, 8, and 24 h of treatment, respectively (Fig. 2B). Thus, Tpen treatment of PCCL3 cells inhibited Tg biosynthesis by approximately 80% and its secretion by 60%-70%, suggesting that zinc depletion inhibits the biosynthesis and secretion of Tg in thyroid cells. Tg is a

660-kDa dimer glycoprotein produced by the thyroid in a TSH-dependent manner. Secreted Tg is a precursor protein essential for thyroid hormone synthesis. After combining with iodine in the follicle colloid, Tg is proteolyzed in the endocytosis process. As a result, T₃, which contains three iodine atoms, and T₄, which contains four iodine atoms, are produced and enter the bloodstream [27,28]. The most important function of T₄ is to promote the cell consumption of oxygen, which stimulates the metabolism in nearly all cells of the body [29]. Excessive production of T₄ causes hyperthyroidism, whereas T₄ deficit leads to hypothyroidism. We performed ELISA analyses of T₄ levels secreted in the cell culture medium to confirm the results of Fig. 2A and 2B. Zinc depletion induced a 20%-30% reduction of T₄ amounts released by PCCL3 cells in the medium, most likely as a result of the inhibition of Tg biosynthesis and secretion (Fig. 2C). Methimazole inhibits the iodination of Tg and is widely used as a treatment for hyperthyroidism [43]. As shown in Fig. 2C, secreted T₄ levels were decreased to nearly the same levels as those obtained upon zinc depletion induced by Tpen. These results clearly showed that zinc depletion inhibited the

biosynthesis and secretion of Tg, likely resulting in insufficient secreted T₄ amounts and lower thyroid activity than normal. The thyroid gland consists of many follicles. Each follicle is bounded by a simple cubic epithelium, but the epithelium of the physiologically active thyroid gland is a simple columnar epithelium [44]. The follicle structure is essential for the good functioning of the thyroid. Here, histological analyses revealed that the follicle structure in a Tpen-treated thyroid was smaller and dented than normal follicles (Fig. 2D), indicating that Tpen affected thyroid functions.

Recently, ER stress has been closely linked to apoptosis and autophagy induction [45]. Several studies have shown that autophagy and apoptosis are induced by zinc release to maintain cell homeostasis and inhibit pathogenesis [46,47]. We investigated whether autophagy or apoptosis was activated upon zinc depletion. Coiled-coil moesin-like Bcl2 interacting protein (Beclin) plays an important role in autophagy and cell death. Apoptosis is activated by the pro-apoptosis protein B-cell lymphoma 2 (Bcl-2)-associated X (Bax) and inhibited by the anti-apoptosis protein Bcl2 [48]. Fig. 3A shows that zinc depletion increased Bax gene expression by about 1.8 times (5 μ M Tpen for 8 h) but did not affect Bcl2 and Beclin. Fig. 3B shows apoptotic bodies observed after Hoechst 33342 staining of cells treated with Tpen. Therefore, apoptosis, but not autophagy, was induced by zinc depletion.

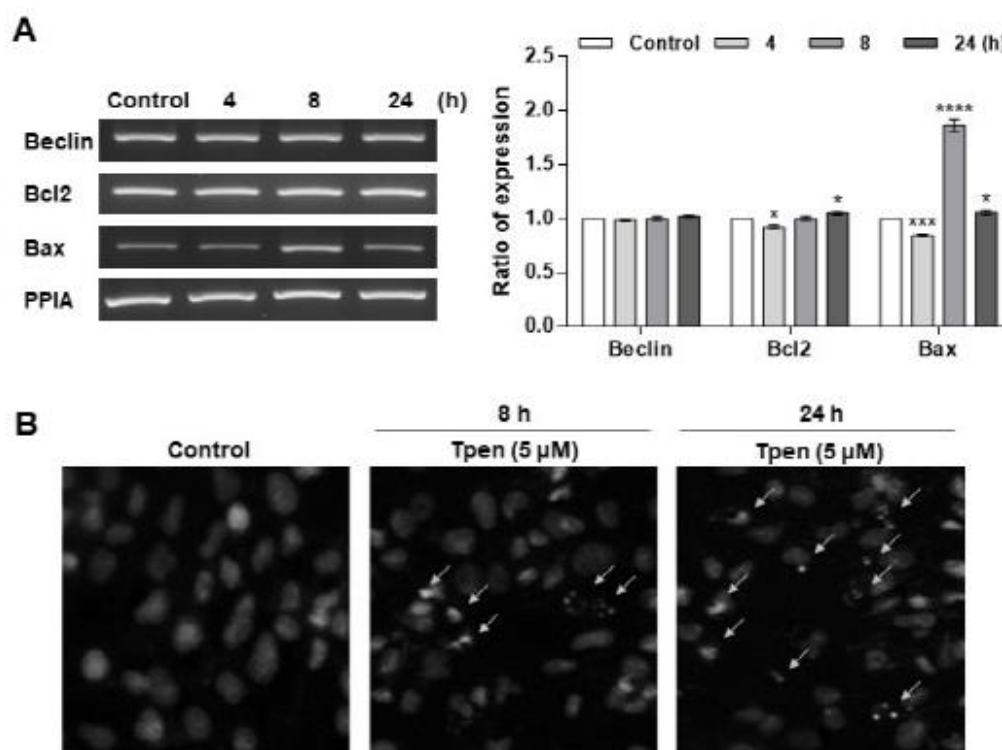


Figure 3. Tpen induces apoptosis. (A) Beclin, Bcl2, and Bax mRNA levels after Tpen treatment. The mRNAs used were the same as those used in Fig. 1C subjected to RT-PCR. (B) Tpen inducible apoptotic bodies as detected by Hoechst 33342 staining. Stained nuclei (arrows) were observed under a fluorescence microscope using a blue filter ($\times 200$). Data represent mean \pm standard error of the mean, n = 6, *p < 0.05, **p < 0.005, ***p < 0.001, ****p < 0.0001 compared with controls.

In summary, we determined the effect of Tpen concentrations and treatment times on PCCL3 thyroid cells' viability. In most experiments, Tpen was used at 8 μ M for 8 h. Zinc depletion did not affect ER chaperones (BiP and PDI) expression but increased the levels of three ER transmembrane signaling proteins (PERK, IRE1, and ATF6). As a result, PERK, IRE1, and ATF6 activated their targets, namely, PERK induced eIF2- α phosphorylation, IRE1 led to XBP1 mRNA splicing, and ATF6 was fragmented. Zinc depletion inhibited both the expression and secretion of Tg, the main precursor of thyroid hormones, in thyroid PCCL3 cells. As a result, the amounts of T4 secreted were 70%-80% of those measured in controls. Additionally, an abnormal follicle structure in the thyroid was detected upon zinc depletion. Finally, zinc depletion induced apoptosis but not autophagy. These data indicate that zinc depletion might cause hypothyroidism by interfering with ER signal pathway and consequently inhibiting Tg expression and secretion. Therefore, maintaining an adequate level of zinc is essential for normal thyroid function. It is required that to changes ER functions in the ER lumen by zinc deletion in further study, it will be given directly how to control Tg secretion through the ER by zinc.

ACKNOWLEDGMENT

This work was supported by the National Research Foundation of Korea (NRF) grant funded by the Korea government (MSIT) (No. NRF-2019R1F1A1049836).

References

[1] N. Roohani, R. Hurrell, R. Kelishadi, R. Schulin. Zinc and its importance for human health: An integrative review. *J Res Med Sci.* 18: 144-157. 2013.

[2] M. Maares, H. Haase. Zinc and immunity: An essential interrelation. *Arch Biochem Biophys.* 611: 58-65. 2016.

[3] Y. Nishi. Zinc and growth. *J Am Coll Nutr.* 15: 340-344. 1996.

[4] S. Tubek, P. Grzanka, I. Tubek. Role of zinc in hemostasis: a review. *Biol Trace Elem Res.* 121: 1-8. 2008.

[5] A.S. Prasad. Impact of the discovery of human zinc deficiency on health. *J Am Coll Nutr.* 28: 257-265. 2009.

[6] S. Vasto, E. Mocchegiani, G. Candore, F. Listi, G. Colonna-Romano, D. Lio, et al. Inflammation, genes and zinc in ageing and age-related diseases. *Biogerontology* 7: 315-327. 2006.

[7] C.P. Wong, E. Ho. Zinc and its role in age-related inflammation and immune dysfunction. *Mol Nutr Food Res.* 56(1): 77-87. 2012.

[8] G.J. Fosmire. Zinc toxicity. *Am J Clin Nutr.* 51: 225-227. 1990.

[9] S. Choi, X. Liu, Z. Pan. Zinc deficiency and cellular oxidative stress: prognostic implications in cardiovascular diseases. *Acta Pharmacol Sin.* 39: 1120-1132. 2018.

[10] K. Grüngreiff, D. Reinhold, H. Wedemeyer. The role of zinc in liver cirrhosis. *Ann Hepatol.* 15: 7-16. 2016.

[11] Y.J. Tamura. The role of zinc homeostasis in the prevention of diabetes mellitus and cardiovascular diseases. *J Atheroscler Thromb.* 28: 1109-1122. 2021.

[12] V.F. Jagadeesan, F. Oesch. Effects of dietary zinc deficiency on the activity of enzymes associated with phase I and II of drug metabolism in Fischer-344 rats: activities of drug metabolising enzymes in zinc deficiency. *Drug Nutr Interact* 1988;5: 403-413. 1988.

[13] T.A. Takeda, S. Miyazaki, M. Kobayashi, K. Nishino, T. Goto, M. Matsunaga, et al. Zinc deficiency causes delayed ATP clearance and adenosine generation in rats and cell culture models. *Commun Biol.* 1: 113. 2018.

[14] Z. Xu, E.J. Squires, T.M. Bray. Effects of dietary zinc deficiency on the hepatic microsomal cytochrome P450 2B in rats. *Can J Physiol Pharmacol.* 72: 211-216. 1994.

[15] P.J. Fraker. Roles for cell death in zinc deficiency. *J Nutr.* 135: 359-362. 2005.

[16] Q. Sun, W. Zhong, W. Zhang, Q. Li, X. Sun, X. Tan, et al. Zinc deficiency mediates alcohol-induced apoptotic cell death in the liver of rats through activating ER and mitochondrial cell death pathways. *Am J Physiol Gastrointest Liver Physiol.* 308: G757-766. 2015.

[17] J. Wang, H. Zhao, Z. Xu, X. Cheng. Zinc dysregulation in cancers and its potential as a therapeutic target. *Cancer Biol Med.* 17: 612-625. 2020.

[18] T.S. Nguyen, K. Kohno, Y. Kimata. Zinc depletion activates the endoplasmic reticulum-stress sensor Ire1 via pleiotropic mechanisms. *Biosci Biotechnol Biochem.* 77: 1337-1339. 2013.

[19] H. Olzscha. Posttranslational modifications and proteinopathies: how guardians of the proteome are defeated. *Biol Chem.* 400: 895-915. 2019.

[20] D.S. Schwarz, M.D. Blower. The endoplasmic reticulum: structure, function and response to cellular signaling. *Cell Mol Life Sci.* 73: 79-94. 2016.

[21] C. Hetz, K. Zhang, R.J. Kaufman. Mechanisms, regulation and functions of the unfolded protein response. *Nat Rev Mol Cell Biol.* 21: 421-438. 2020.

[22] J.M.D. Grandjean, R.L. Wiseman. Small molecule strategies to harness the unfolded protein response: where do we go from here? *J Biol Chem.* 295: 15692-15711. 2020.

[23] C. Hetz, F.R. Papa. The Unfolded Protein Response and Cell Fate Control. *Mol Cell* 69: 169-181. 2018.

[24] V.M. Parmar, M. Schröder. Sensing endoplasmic reticulum stress. *Adv Exp Med Biol.* 738: 153-168. 2012.

[25] A. Fribley, K. Zhang, R.J. Kaufman. Regulation of apoptosis by the unfolded protein response. *Methods Mol Biol.* 559: 191-204. 2005.

[26] S.A. Oakes, F.R. Papa. The role of endoplasmic reticulum stress in human pathology. *Annu Rev Pathol.* 10: 173-94. 2015.

[27] D. Braun, U. Schweizer. Thyroid Hormone Transport and Transporters. *Vitam Horm.* 106: 19-44. 2018.

[28] G.A. Brent. Mechanisms of thyroid hormone action. *J Clin Invest.* 122: 3035-3043. 2012.

[29] S.Y. Cheng, J.L. Leonard, P.J. Davis. Molecular aspects of thyroid hormone actions. *Endocr Rev.* 31: 139-170. 2010.

- [30] J.B. Beserra, J.B.S. Morais, J.S. Severo, K.J.C. Cruz, A.R.S. de Oliveira, G.S. Henriques, et al. Relation Between Zinc and Thyroid Hormones in Humans: a Systematic Review. *Biol Trace Elem Res.* 199: 4092-4100. 2021
- [31] M.A. Paulazo, A.J. Klecha, H.A. Sterle, E. Valli, H. Torti, F. Cayrol, et al. Hypothyroidism-related zinc deficiency leads to suppression of T lymphocyte activity. *Endocrine* 66: 266-277. 2019.
- [32] P.S. Kim, O.Y. Kwon, P. Arvan. An endoplasmic reticulum storage disease causing congenital goiter with hypothyroidism. *J Cell Biol.* 133: 517-527. 1996.
- [33] P.S. Kim, S.A. Hossain, Y.N. Park, I. Lee, S.E. Yoo, P. Arvan. A single amino acid change in the acetylcholinesterase-like domain of thyroglobulin 20120causes congenital goiter with hypothyroidism in the cog/cog mouse: a model of human endoplasmic reticulum storage diseases. *Proc Natl Acad Sci USA.* 95(17):9909-9913. 1998.
- [34] G. Medeiros-Neto, P.S. Kim, S.E. Yoo, J. Vono, H.M. Targovnik, R. Camargo, et al. Congenital hypothyroid goiter with deficient thyroglobulin. Identification of an endoplasmic reticulum storage disease with induction of molecular chaperones. *J Clin Invest.* 98: 2838-2844. 1996.
- [35] B. Guantario, A. Capolupo, M.C. Monti, G. Leoni, G. Ranaldi, A. Tosco, et al. Proteomic Analysis of Zn Depletion/Repletion in the Hormone-Secreting Thyroid Follicular Cell Line FRTL-5. *Nutrients* 10:1981. 2018.
- [36] V.L. Bodiga, P.K. Vemuri, G. Nimmagadda, S. Bodiga. Zinc-dependent changes in oxidative and endoplasmic reticulum stress during cardiomyocyte hypoxia/reoxygenation. *Biol Chem.* 401: 1257-1271. 2020.
- [37] Z. Yu, Z. Yu, Z. Chen, L. Yang, M. Ma, S. Lu, et al. Zinc chelator TPEN induces pancreatic cancer cell death through causing oxidative stress and inhibiting cell autophagy. *J Cell Physiol.* 234: 20648-20661. 2019.
- [38] A.S. Prasad. Discovery of human zinc deficiency: its impact on human health and disease. *Adv Nutr.* 4: 176-190. 2013.
- [39] C.T. Walsh, H.H. Sandstead, A.S. Prasad, P.M. Newberne, P. Fraker. Zinc: health effects and research priorities for the 1990s. *J Environ. Health Perspect.* 102 Suppl 2: 5-46. 1994.
- [40] W. Rozpedek, D. Pytel, B. Mucha, H. Leszczynska, J.A. Diehl, I. Majsterek. The role of the PERK/eIF2alpha/ATF4/CHOP signaling pathway in tumor progression during endoplasmic reticulum stress. *Curr Mol Med.* 16: 533-544. 2016.
- [41] R.F. Hillary, U. FitzGerald. A lifetime of stress: ATF6 in development and homeostasis. *J Biomed Sci.* 25: 48. 2018.
- [42] Y. Chen, F. Brandizzi. IRE1: ER stress sensor and cell fate executor. *Trends Cell Biol.* 23: 547-555. 2013.
- [43] H. Abdi, A. Amouzegar, F. Azizi. Antithyroid drugs. *Iran J Pharm Res.* 18(Suppl1):1-12. 2019.
- [44] J. Lee, S. Yi, Y.E. Kang, H.W. Kim, K.H. Joung, H.J. Sul, et al. Morphological and Functional changes in the thyroid follicles of the aged murine and humans. *J Pathol Transl Med.* 50: 426-435. 1996.
- [45] S. Song, J. Tan, Y. Miao, M. Li, Q. Zhang. Crosstalk of autophagy and apoptosis: Involvement of the dual role of autophagy under ER stress. *J Cell Physiol.* 232: 2977-2984. 2017.
- [46] S.N. Bae, K.H. Lee, J.H. Kim, S.J. Lee, L.O. Park. Zinc induces apoptosis on cervical carcinoma cells by p53-dependent and -independent pathway. *Biochem Biophys Res Commun.* 484: 218-223. 2017.
- [47] J.P. Liuzzi, R. Pazos. Interplay between autophagy and zinc. *J Trace Elem Med Biol.* 62: 126636. 2020.
- [48] F. Edlich. BCL-2 proteins and apoptosis: Recent insights and unknowns. *Biochem Biophys Res Commun.* 500: 26-34. 2018.

Conflicts of Interest: The authors declare no conflicts of interest.

Contribution of Individual Authors to the Creation of a Scientific Article (Ghostwriting Policy)

Seung-Whan Kim, O-Yu Kwon: Conceptualization, Resources, Supervision, Project administration, Writing Original Draft. **Tae-Sik Hwang, Hyewon Park, Eun-Ryeong Lee:** Methodology, Investigation, Writing - Original Draft. **Kisang Kwon, Kyung-Hee Kang:** Review & Editing, Visualization.

Sources of Funding for Research Presented in a Scientific Article or Scientific Article Itself

This work was supported by the National Research Foundation of Korea (NRF) grant funded by the Korea government (MSIT) (No. NRF-2019R1F1A1049836).

Creative Commons Attribution License 4.0 (Attribution 4.0 International, CC BY 4.0)

This article is published under the terms of the Creative Commons Attribution License 4.0 https://creativecommons.org/licenses/by/4.0/deed.en_US